1. Michelson - Stellar Interferometer, Error Budget for Triple Satellite Configuration

2. Performance Report

3. Principal Investigator: Arvind S. Marathay

4. Period Covered: Feb. 95 - Jan. 31, 1996

5. Optical Sciences Center
University of Arizona
Tucson, AZ 85721

6. NASA Grant NAG5-2427

J. Shiefman, B. Bos, A. S. Marathay
Optical Sciences Center, University of Arizona, Tucson, AZ 85721

This is our performance report. In September '95 we presented a paper at the Optical Society of America, Annual Meeting in Portland. Much has transpired since our last report. Joe attended the meeting and the talk went well. There was much interest displayed by the audience as indicated by the questions after the talk and subsequent discussions afterwards with audience members. He met several participants in active stellar interferometry projects.

See Itemized List of Project Components. All of the items in section II (verify model for the conventional MSI) from our itemized list of project components in our May 30 monthly report (a copy of this list has been enclosed in this report) have been completed successfully (except for items II C, the 2-D source, which we previously put on hold and item II H, asymmetrical mirror placement, which rightfully belongs in section V, which is devoted to examining instrument tolerances. We now feel confident that we have a program that will accurately model the conventional MSI system.

In order to reach this stage we have finished a program that calculates and plots phase as a function of baseline. The bottom plot in figure 1 shows a plot of fringe phase versus baseline for a source with a rectangular radiance distribution. We have also added variable delay lines to both arms of the interferometer (see system drawing labeled figure 2). We have also completed a program that calculates visibility as a function of both baseline and OPD for polychromatic sources. Figure 3 shows a 3-D plot from this program. One of the variable axes is baseline running from 5 to 50 meters. The other variable axis OPD with the zero OPD point in the center of the axis. The response variable (visibility) is plotted on the vertical axis from approximately zero to 0.94. Both the spatial and spectral distributions of the source are rectangular and therefore show sinc function dependence on baseline and OPD respectively.

Rather than starting the new model for the "modern" MSI (item III from the list of project components) we decided to start testing the effect of instrument errors on visibility and phase for the conventional MSI (item V from the list). This path seemed to make more sense and it also provided some results for us to report at the Portland meeting. To date we have investigated the effects on visibility and phase due to several types of instrument errors.

We have finished modeling the effects of mirror tilts (item V A), both in an ASAP model and in parallel analytical calculations. The most interesting effects of mirror tilt for our type of application show up as errors in the phase of the measured fringes. This error arises because the optical path lengths of the beams in the arm with the tilted mirror are changed (usually increased) relative to the beams in the other arm of the

interferometer. This in turn causes a shifting of the zero OPD fringe. This effect is shown in figure 4 with a drawing that shows how a tilt of one of the inner mirrors by an angle α cause a path length error to accumulate as the beam propagates from the inner mirror to the slit. The equation below the drawing shows how to calculate the induced path length error. It is interesting to notice in the drawing that this tilt induced phase error gets magnified greatly by the 10X afocal telescope due to the 10X angular magnification. In fact, as the equation on the bottom of figure 4 indicates that there is a quadratic dependence between the tilt angle and the generated path length error. Therefore, the 10X afocal telescope cause 100X the error per unit length of travel. For this reason, it would increase system tolerances to make the afocal telescope as compact in length as possible. This would probably increase the design complexity and cost of the afocal telescopes. Figure 5 shows a plot of phase shift error as a function of inner mirror tilt angle. This plot shows the quadratic dependence referred to previously. The plot in figure 5 was for a system with 5 meters between the inner mirror and the slit, with 3.5 meters of that space filled by a 10X afocal telescope.

The visibility can be influenced by mirror tilt in two different ways. The first way would involve a large enough tilt to cause the beam to be decentered about the slit by an amount sufficient to cause a portion of the slit to not be illuminated (the slit is intended to be overfilled). Because less light would reach the fringe plane from the arm with the mirror tilt than from the arm without the mirror tilt, a loss of visibility due to the unequal intensities in the two arms would then result. Although the sensitivity to this type of error is increased as the afocal telescope length increases, just as it did in the case of the phase error, in the visibility case it is easy to build the system so that it would take a relatively large mirror tilt to cause any of the light to miss the slit. Therefore, loss of visibility of this type is relatively easy to eliminate. The second way that mirror tilt effects visibility is due to the fact that the amount of change in path length caused by the mirror tilt is slightly different for the beams from each source point. This causes the zero OPD fringe of each of the source points to shift by a slightly different amount, which will in turn lead to a change in the visibility. For the small angular subtense astronomical objects that we typically look at with the MSI these changes in visibility are negligible.

We tested the effect of unequal intensities in the two arms (item V C). This showed the expected visibility change by a multiplicative factor of $2\sqrt{I_1}\, I_2/(I_1+I_2)$ and no change in the phase.

We changed the OPD in one arm by varying the amount of delay in that arm (item V D). This showed a constant shift of the fringes appropriate for the amount of path length change in the delay line as given by the equation $\Delta\Phi = (2\pi/\lambda) * \Delta l$.

We examined the effect of an object tracking error (i.e. an off-axis object) and found that it produced a phase shift that is linear with baseline. Figure 6a shows a plot of phase shift as a function of baseline for an off-axis source with a rectangular radiance distribution like the one shown in figure 6b (note: the π radians phase jump at a baseline

value of about 35 meters is due to the phase reversal that takes place when the sinc function goes through zero). As indicated in figure 6b the phase shift increases by 2 π whenever the baseline increases by amount equal to λ/β where λ is the wavelength and β is the angular shift of the object center off of the optical axis. The tracking error causes no change in visibility.

We have also generated results but not completed studying the effects due to items E, mirror flatness (the deviation from flatness was created by adding various amounts of Zernike polynomials to the mirror surfaces), F, mirror surface roughness, and scattering in the system (something that we didn't include in the May 30 report sent to the technical officer Bernie D. Seery).

We now have a fully tested and operational computer model of the conventional MSI. We are continuing to test the model to obtain the system tolerances.

SYSTEM MODEL VERIFICATION
SOURCE PROPERTIES

METRICS: VISIBILITY & PHASE

PLOTS FOR SOURCE WITH RECTANGULAR RADIANCE APODIZATION

Visibility vs. Baseline

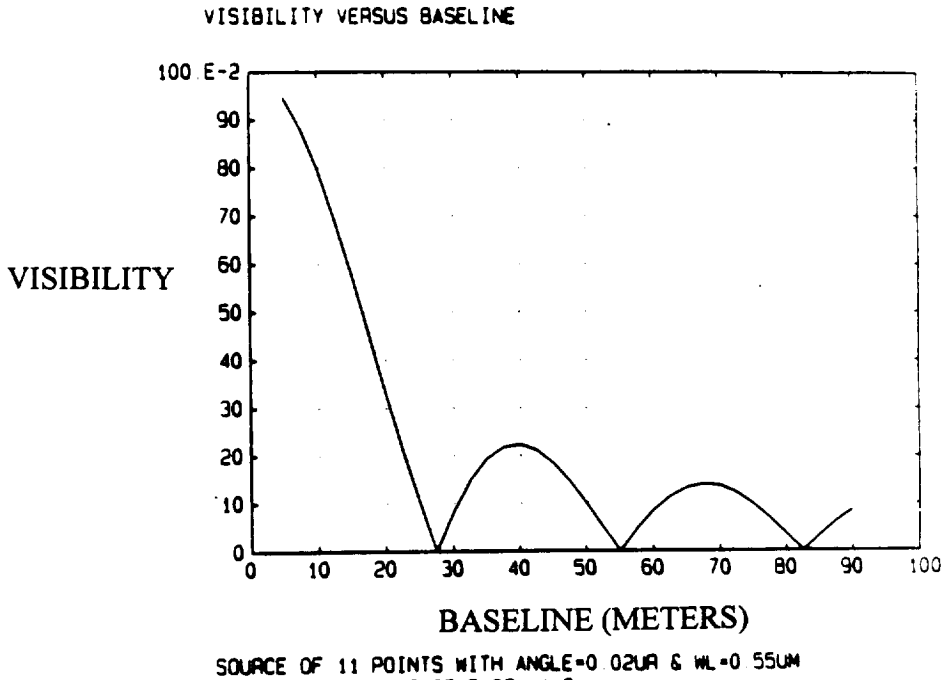

Phase vs. Baseline

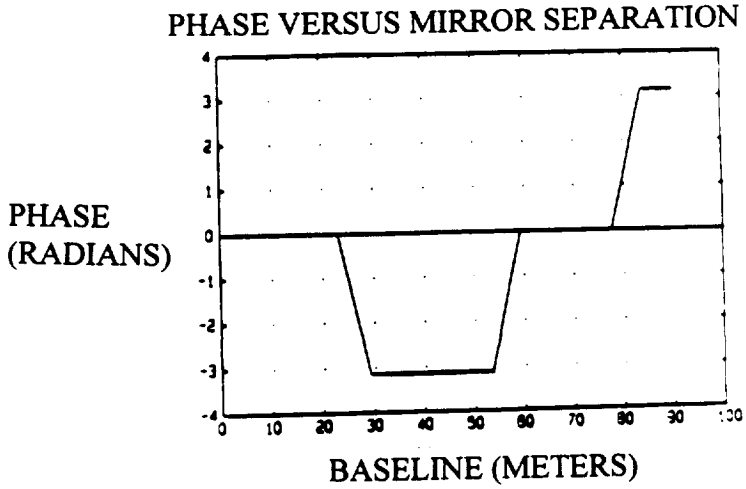

FIGURE 1

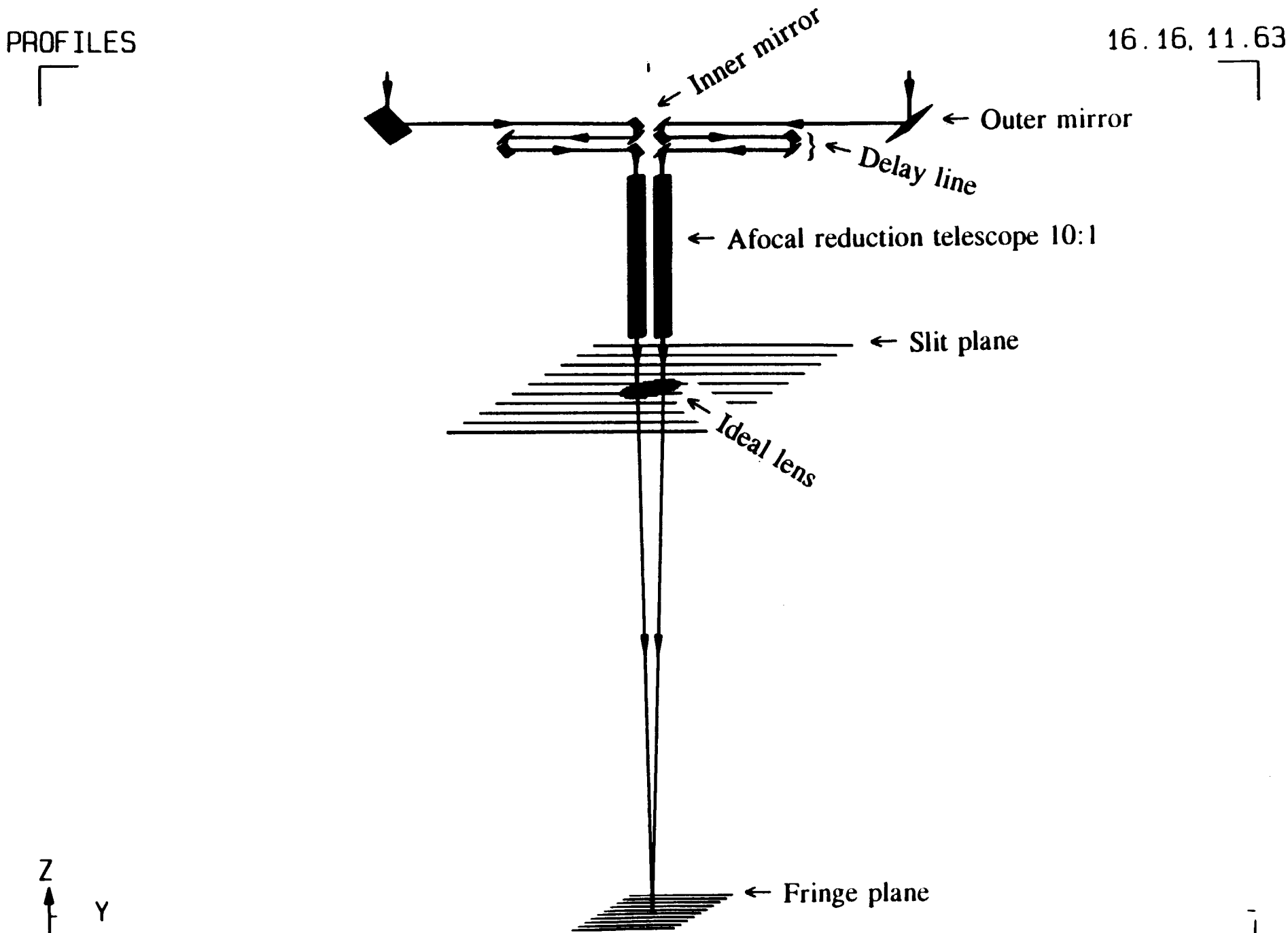
PROFILES
16.16, 11.63
Inner mirror
Outer mirror
Delay line
Afocal reduction telescope 10:1
Slit plane
Ideal lens
Fringe plane
Z
Y
X
-.9226, -11.63, .2384E-6
ASAP v4.0
08/28/95 21:19

FIGURE 2

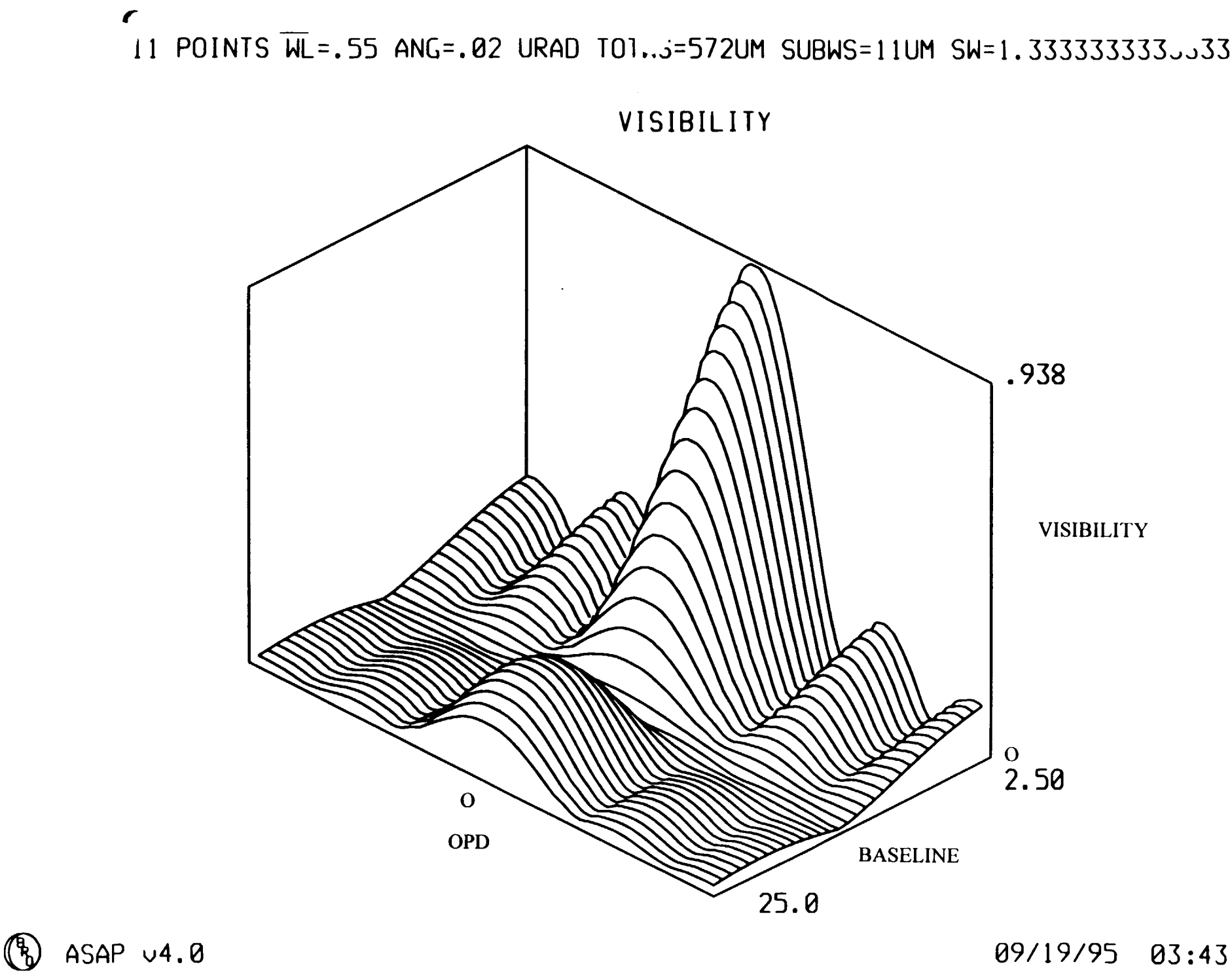
11 POINTS WL=.55 ANG=.02 URAD TOT..3=572UM SUBWS=11UM SW=1.333333333333333
VISIBILITY
.938
VISIBILITY
0
2.50
0
OPD
BASELINE
25.0
ASAP v4.0
09/19/95 03:43

FIGURE 3

INSTRUMENT TOLERANCE RESULTS

- MIRROR TILT

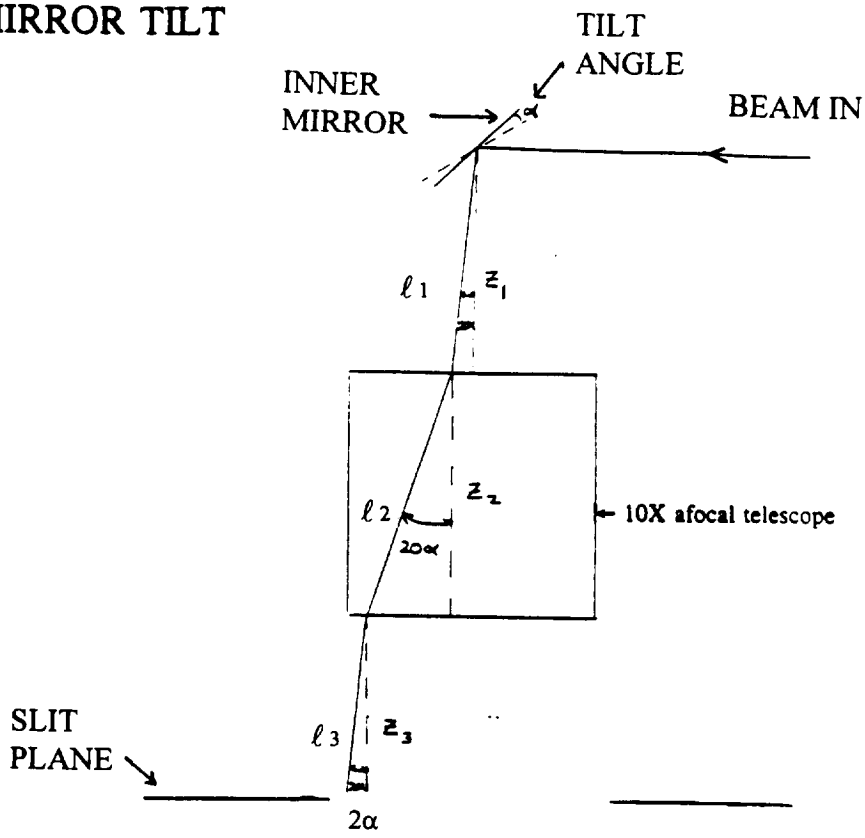

$$OPD_{TOTAL} = (\ell_1 - Z_1) + (\ell_2 - Z_2) + (\ell_3 - Z_3)$$

$$= Z_1\left(\frac{1}{\cos(2\alpha)} - 1\right) + Z_2\left(\frac{1}{\cos(20\alpha)} - 1\right) + Z_3\left(\frac{1}{\cos(2\alpha)} - 1\right)$$

AFOCAL EFFECT ~100X PER UNIT LENGTH

$$\frac{1}{\cos(2\alpha)} - 1 \approx 2\alpha^2 \qquad \frac{1}{\cos(20\alpha)} - 1 \approx 200\alpha^2$$

FIGURE 4

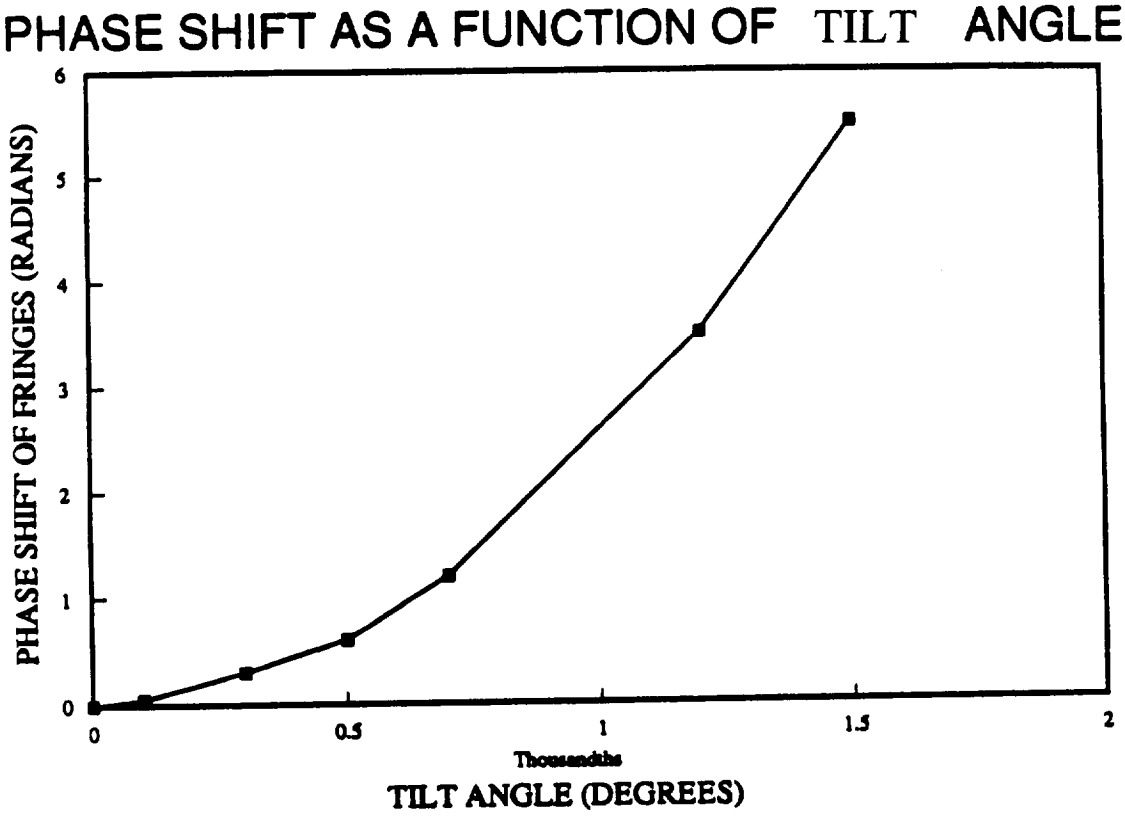
PHASE SHIFT AS A FUNCTION OF TILT ANGLE
PHASE SHIFT OF FRINGES (RADIANS)
0
1
2
3
4
5
6
0
0.5
1
1.5
2
Thousandths
TILT ANGLE (DEGREES)

FIGURE 5

INSTRUMENT TOLERANCE RESULTS

- TRACKING ERROR

Phase vs. Baseline for off-axis object with rectangle radiance apodization

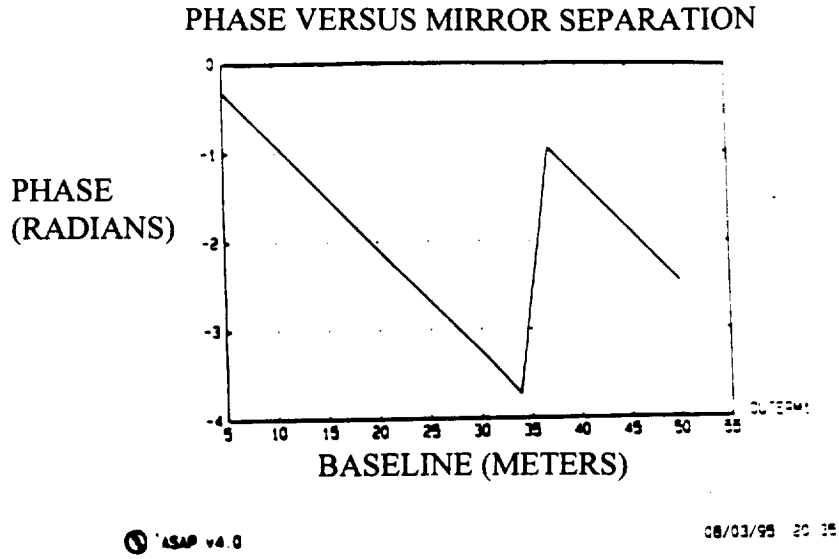

FIGURE 6a

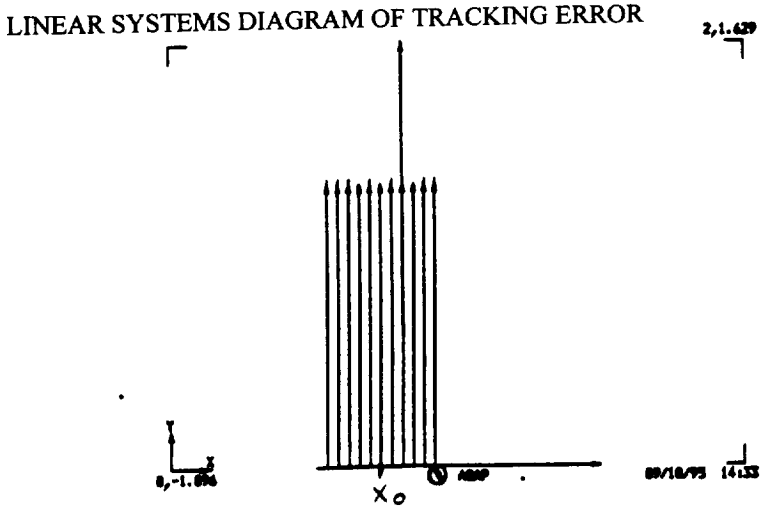

$$\Delta\phi = 0, 2\pi, 4\pi, \ldots$$

$$\textit{FOR } B = 0, \frac{\lambda}{\beta}, \frac{2\lambda}{\beta}, \ldots$$

WHERE β IS THE ANGULAR SHIFT OF THE OBJECT CENTER

FIGURE 6b